Balancing circuit new control for supercapacitor storage system lifetime maximization

Seima Shili [a], Alaa Hijazi [b], Ali Sari [a], Xuefang Lin-Shi [b], Pascal Venet [a]

(a) Laboratoire Ampère, UMR CNRS 5005 Université de Lyon, Université Claude Bernard Lyon 1, 43 bd du 11 novembre 1918, Bât. Omega Villeurbanne, F-69622 Cedex, France.

(b) Laboratoire Ampère, UMR CNRS 5005 Université de Lyon, INSA de Lyon, 21 av. Jean Capelle, Bât. Léonard de Vinci Villeurbanne, F-69621 Cedex, France.

Abstract— Energy storage elements such as supercapacitors are widely used in high power applications. However, due to single cell voltage limitation, an energy storage system with large number of supercapacitors is often employed. Energy management systems are associated to energy storage systems in order to assure user and equipment safety. Balancing circuits, which enable the equalization of the voltage of each element in series, are a part of energy management system device. The work presented in this paper aims to enhance the lifetime of energy storage systems. It relies on better controlling balancing circuits on the terminals of the storage system elements. With the conventional function of balancing circuit, the energy storage system is limited by its weakest element which may fail prematurely. Thus, a new balancing approach is presented, discussed and analyzed. It is based on the elements degradation level prediction. The model predictive control used with the new approach, aims to equalize aging speed between elements of a module and ensures a maximum lifetime to the energy storage system. A comparison with the conventional control, shows that adopting this new approach, with the same equipment, can enhance the storage system's lifetime by dozens percent.

Index Terms— Balancing circuit, Battery Management System (BMS), Electrochemical Double Layer Capacitor (EDLC), State Of Health (SOH), supercapacitor.

I. INTRODUCTION

Electrochemical double layer capacitors (EDLC) [1], generally referred to supercapacitors or ultracapacitors [2][3][4][5], are employed in many areas such as transport applications and un-interruptible power supply. In fact, they offer multiple advantages when compared to other energy storage systems [6]. They are characterized by their low series resistances, high power densities, good performances in low temperatures and relatively high cycle lives [7][8]. This explains their usage in devices that supply or recover high pulse power [9][10][11][12]. In several applications, the voltage of the energy storage system is significantly higher than the voltage of a single cell which is limited to 3V. Therefore, a large number of supercapacitors is stacked in a module, called supercapacitor energy storage system (SESS), in order to reach the required value of the voltage [13].

Similarly to electrochemical batteries, energy management is essential for security and reliability reasons. Battery management system (BMS) is the most widespread appellation of those energy management systems [14][15]. However, other appellations also exist in the market. Supercapacitor manager (SCM) is used in the following to avoid the confusion with battery energy storage systems. Generally, this system protects the storage module from damage and maintains it in accurate and reliable operational conditions. In fact, it performs several tasks such as voltage and temperature monitoring, states estimation (state of charge…), thermal management, safety management, and balancing. Its functions are based on measuring some variables like voltage, current and temperature.

This paper develops the balancing function of the SCM in order to enhance the lifespan of the supercapacitor energy storage system.

Balancing function aims to equalize voltage between SESS elements using balancing circuits. This equalization is compulsory for energy storage systems. Indeed, voltage differences between same module elements are obviously present and increase during operation due to intrinsic and environmental causes. Intrinsic causes concern manufacture tolerance and initial characteristic differences between same types of supercapacitor while environmental causes are mainly the thermal dispersion across the pack. Balancing function resolves the issue of voltage inequality. Methodologies used to balance the cell voltage in a supercapacitor energy storage system are categorized into dissipative and redistributive (or non-dissipative) [16][17] . Dissipative balancer removes the excess charge from the higher charged cells through a balancing circuit resistor. Redistributive balancing circuit removes charge from higher energy cell or cells and transfers it to the lower charged ones. Energy transfer is assured by using various circuit designs employing capacitors, inductors and/or converters [18][19][20][21]. The redistributive balancing circuit is very beneficial. However, the dissipative one remains widely present in the marketplace due to its simplicity and low cost [22][23][24]. For supercapacitor energy storage systems, dissipative equalization method is the only technique existing in the market today.

The work presented in this paper explores the dissipative balancing circuit also known as the switched shunt resistor or controlled shunting resistor. This circuit is composed of a resistor associated to a switch and connected in parallel to each cell. When the imbalance occurs, the classical on-off switch control dissipates energy, protects cells from over-charging and minimizes global voltage dispersion inside the pack [16].

This classical balancing control strategy only takes the voltage dispersion into account. However, temperature is an important aging factor and should not be neglected when balancing the cells. Some experiment results show that temperature differences between same pack elements can reach up to 10 °C [25]. Then, if voltage equalization is established without temperature considerations the system will suffer from state-of-health imbalances and cell failures.

This paper proposes a new balancing circuit control strategy that considers cell voltage, temperature and aging dispersion in order to maximize the lifespan of the whole storage system. The model predictive control tool includes this new strategy. Unlike classical equalization, the new control approach doesn't aim to equalize voltages but equalizes the speed of degradation of each cell. It will produce voltage dispersion that compensates the aging differences inside the energy storage pack. Indeed, the more the cell is degraded, the less it is solicited and reciprocally.

The remainder of the paper is organized as follows. Section II reviews the supercapacitor aging behavior in order to explain the aging model. The predictive control is based on this model. Section III describes the new model predictive control of the balancing circuit and the objectives of the lifetime maximization. Section IV presents realistic simulation using Matlab/Simulink to demonstrate the good performance of the new control approach. Finally, section V summarizes the simulation results and compares them to classical voltage equalization under same operating conditions.

II. System Aging Behavior

This section introduces the supercapacitor aging behavior in order to understand the lifetime evolution of the energy storage system and the benefit of the model presented.

A. Supercapacitor aging behaviour

Lifetime of supercapacitors is limited. Their energy storage mechanism is theoretically electrostatic, electrochemical reactions unfortunately exist. They correspond mainly to residues of acidic or organic chemicals used for digging porosity in pure carbon during the activation process. Those parasitic species are reactive under supercapacitor voltage and temperature. They lead to solid and gases products that participate in the aging process of the supercapacitor. The aging mechanisms are principally the loss of usable energy storage surface and the increase of pressure inside the supercapacitor. The loss of usable energy storage surface causes the decrease of capacitance through time. Moreover, the pressure increase causes electrode cracks and supercapacitor packaging lengthening which damages the collectors [26].

Thus, the aging phenomena leads to a loss of capacitance (loss of energy storage surface) and an increase of resistance (decrease of the mobility of ions in the separator because of trapped gases and contacts damages with overpressure) [27][28][29]. Classical end of life criteria are generally defined as the loss of 20 % of the initial capacitance and the double of the initial equivalent series resistance. Consequently, the cells inside the pack have different ages depending on the temperature, voltage and cycling stresses they have experienced. The pack end of life is defined when the weakest cell reaches one of its end of life criteria [30].

B. Supercapacitor degradation law

The classical aging model for supercapacitors is Eyring's law that estimates the aging rate. This law stipulates that a 200 mV voltage surplus increases the aging by a factor of 2 and have the same effect as a temperature increase of 10 °C [25].

Research on high power cycling test reported that the storage element aging behavior is also affected by the type of cycling [31][32][33].

Therefore, the model chosen to represent a supercapacitor aging incorporates power cycling effect in the classical Eyring's model. The lifetime of the supercapacitor τ_d taking into account cell voltage, temperature and RMS current over a time laps is then expressed by (1) [25].

$$\tau_d = \tau_0 \cdot \frac{T}{\int_{t_f}^{t_i} \exp\left(\frac{V(t)}{V_0} + \frac{\theta(t)}{\theta_0} + \frac{I_{RMS}}{I_{RMS\,0}}\right) dt} \qquad (1)$$

Where, $V(t)$, $\Theta(t)$ and I_{RMS} are voltage, temperature and RMS current. τ_0, V_0, Θ_0 and I_{RMS0} are constants. t_f and t_i are the final time and the initial time of a period T.

According to the classical end of life criteria, during this estimated lifetime, supercapacitor capacitance and equivalent series resistance are supposed to start by their initial values ($C(0)$ and $ESR(0)$) and evolve until reaching their final values $0.8 \cdot C(0)$ and $2 \cdot ESR(0)$.

III. New Predictive control approach for balancing circuit

Finite Control Set Model predictive control (FCS-MPC) is an advanced popular tool used in many fields. Its principle is based on the predictive discrete-time model of the system [34]. At each sample time, it predicts the system response for the finite set of switching states of control. The switching state that minimizes a user defined cost function is selected. Thanks to this updated prediction strategy, the control simplicity and efficiency of the FCS-MPC have been demonstrated to be strong [9][35][36].

In this section, the predictive model and the control objectives formulated as a maximizing cost function are described.

A. System description

Consider a supercapacitor energy storage pack composed of n supercapacitors placed in series and n switched shunt resistors placed at the terminal of each cell as a balancing circuit. The electrical model chosen to represent a supercapacitor is the series connection between a capacitance C and a resistance ESR (Equivalent Series Resistance). Despite the simplicity of the model, it is sufficient to represent the required electrical and aging behavior of the cell. Indeed, as mentioned before, the capacitance C and the resistance ESR are the two electrical parameters changing with age. The n switches S_i (usually MOSFET) are controlled in order to maximize the lifespan of the whole storage system (see Fig.1).

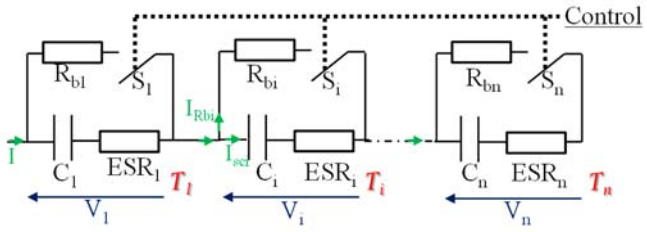


Fig. 1. Energy storage system and its balancing circuits, C_i: cell capacitor, ESR_i: cell equivalent series resistance, V_i: cell voltage, T_i: cell temperature, R_{bi}: balancing circuit resistance, S_i: balancing circuit switch.

B. Predictive model

The aim of the predictive model is to predicate the lifetime of the system. This goal is achieved by representing the relationship between the balancing circuit control and the aging of the cell.

The following introduces the modeling steps.

When i^{th} balancing circuit is activated ("On" state), it transfers a part of the cell input current into its balancing resistor and dissipates energy. When it is disabled ("Off" state), the total input current passes through the cell.

For i = 1…n, the i^{th} storage element instant voltage is given by (2) (see Fig. 1).

$$V_i(t) = V_{Ci0} + \frac{1}{C_i(t)} \int I_{sci}(t)dt + ESR_i(t) \cdot I_{sci}(t) \qquad (2)$$

$$I_{sci}(t) = I(t) - (S_i(t) \cdot \frac{V_i(t)}{R_b}) \qquad (3)$$

Where, V_{Ci0}, $C_i(t)$ and $ESR_i(t)$ are the initial voltage, the actual capacitance and ESR of the i^{th} supercapacitor respectively, $I_{sci}(t)$ is the current through the i^{th} supercapacitor and I(t) is the storage system input current. Same balancing circuit for each element on the whole storage system is considered. Therefore, the balancing resistor values are all equal to R_b.

$S_i(t)$ represents the i^{th} current of the supercapacitor balancing circuit MOSFET sequence, where,

$S_i(t) = 0$ if i^{th} MOSFET is "Off"

$S_i(t) = 1$ if i[th] MOSFET is “On”

Therefore, equation (2) becomes:

$$V_i(t) = V_{Ci0} + \frac{1}{C_i(t)} \int \left(I(t) - (S_i(t) \cdot \frac{V_i(t)}{R_b}) \right) dt + ESR_i(t) \cdot \left(I(t) - (S_i(t) \cdot \frac{V_i(t)}{R_b}) \right) \quad (4)$$

Then:

$$\frac{dV_i(t)}{dt} = \frac{d\left(\frac{1}{C_i(t)} \int \left(I(t) - (S_i(t) \cdot \frac{V_i(t)}{R_b}) \right) dt \right)}{dt} + \frac{d\left(ESR_i(t) \cdot \left(I(t) - (S_i(t) \cdot \frac{V_i(t)}{R_b}) \right) \right)}{dt} \quad (5)$$

While,

$$\frac{dV_i(t)}{dt} = \frac{V_i(t+dt) - V_i(t)}{dt} \quad (6)$$

$ESR_i(t)$, $C_i(t)$, $S_i(t)$ and $I(t)$ are constant during *dt*. Therefore, equation (5) becomes:

$$\frac{dV_i(t)}{dt} = \frac{1}{C_i} \left(I - (S_i \cdot \frac{V_i(t)}{R_b}) \right) - \left(ESR_i \cdot \frac{S_i}{R_b} \cdot \frac{dV_i(t)}{dt} \right) \quad (7)$$

Consequently,

$$V_i(t+dt) = \left(\frac{1}{C_i} \cdot \left(\frac{R_b}{R_b + ESR_i \cdot S_i} \right) \right) \cdot I \cdot dt + \left(1 - \frac{dt \cdot S_i}{C_i \cdot (R_b + ESR_i \cdot S_i)} \right) V_i(t) \quad (8)$$

The dynamic of the i[th] supercapacitor voltage is represented by a discrete time model (9):

$$V_i(k+1) = \left(\frac{1}{C_i} \cdot \left(\frac{R_b}{R_b + ESR_i \cdot S_i} \right) \right) \cdot I \cdot ts + \left(1 - \frac{tp \cdot S_i}{C_i \cdot (R_b + ESR_i \cdot S_i)} \right) V_i(k) \quad (9)$$

S_i represents the i[th] switch control state, k∈N denotes the discrete time step, ts is the sample time, R_b is the balancing resistor value, C_i is the i[th] cell capacitance, ESR_i is the i[th] cell ESR and $V_i(k)$ is the i[th] cell voltage at k.

The second modeling step is the prediction of the supercapacitor lifetime using the voltage model prediction.

The discretization of the lifetime defined by (1) $\tau_{di}(k)$ is expressed by (10).

$$\tau_{di}(k) = \tau_0 \cdot \frac{1}{\frac{ts}{T_w} \sum_{j=k-\frac{Tw}{ts}}^{j=k} \exp\left(\frac{V_i(j)}{V_0} + \frac{\theta_i(j)}{\theta_0} + \frac{I_{RMS}}{I_{RMS\,0}} \right)} \quad (10)$$

$\tau_{di}(k)$ is the i[th] supercapacitor lifetime taking into account the cell voltage, temperature and RMS current over running window T_w, ($T_w = \alpha \cdot ts$ with α a constant).

Thus in (11), the predictive lifetime over the running window T_w points includes the predictive voltage (9) with the switched control state.

$$\tau_{di}(k+1) = \tau_0 \cdot \frac{1}{\frac{ts}{T_w}\sum_{j=k+1-\frac{T_W}{ts}}^{j=k+1} \exp\left(\frac{V_i(j)}{V_0} + \frac{\theta_i(j)}{\theta_0} + \frac{I_{RMS}}{I_{RMS\,0}}\right)} \quad (11)$$

The dynamic of the cell's temperature is much slower than the dynamic of the voltage [37]. Therefore, the temperature is supposed to be constant between two consecutive discrete times (12).

$$\theta_i(k) = \theta_i(k+1) \quad (12)$$

The next modeling step is the prediction of the supercapacitor aging behavior. As mentioned before, it is related to capacitance or ESR deterioration. Thus, the evolution of the parameters of the balancing control is modeled as a predictive model in order to monitor supercapacitor's aging behavior. Experiments show that supercapacitor's ESR and C deterioration evolves simultaneously [38][39][40]. Thus, prediction of one of these parameters is sufficient for aging monitoring. In this case, the prediction involves the ESR evolution. The ESR predictive evolution is inspired from linear evolution of ESR at specific voltage temperature and current solicitation [25][41][42].

Figure 2 schematizes the ESR_i evolution. At every step time tp, the equivalent series resistance increases linearly to reach its following value. The linear evolution from one step to another depends on the supercapacitor solicitations (voltage, temperature and RMS current). Indeed, during a period of time, indication about cell temperature, voltage and RMS current provides the corresponding lifetime of the supercapacitor $\boldsymbol{\tau}_{di}$. This lifetime represents the time that the initial ESR ($ESR_i(0)$) reaches linearly its end of life criterion, ($2 \cdot ESR_i(0)$). Thus, actual $ESR_i(k)$ evolves to $ESR_i(k+1)$ during tp. Similarly, $ESR_i(0)$ evolves to $2 \cdot ESR_i(0)$ during $\boldsymbol{\tau}_{di}(k)$ (13). This is represented by the lines having the same slope.

$$ESR_i(k+1) = ESR_i(k) + \left[\frac{ESR_i(0)}{\tau_{di}(k)} \cdot tp\right] \quad (13)$$

The ESR predictive evolution model according to the cell lifetime is presented by equation (14). This equation presents $ESR_i(k+2)$ in function of the current $ESR_i(k)$ and includes the lifetime model prediction.

$$ESR_i(k+2) = ESR_i(k+1) + \left[\frac{ESR_i(0)}{\tau_{di}(k+1)} \cdot tp\right] \quad (14)$$

Where,

$$ESR_i(k+2) = ESR_i(k) + \left[\frac{ESR_i(0)}{\tau_{di}(k)} \cdot tp\right] + \left[\frac{ESR_i(0)}{\tau_{di}(k+1)} \cdot tp\right] \quad (15)$$

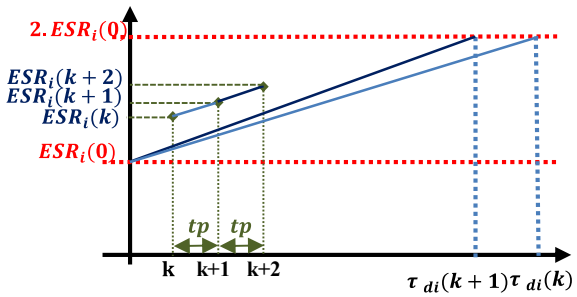


Fig. 2. ESR evolution principle

The same approach can be also applied for the monitoring of the capacitance that would decrease from its initial value $C_i(0)$ to 80% of $C_i(0)$.

The final modeling step is the cell state of aging prediction. The cell state of health (SOH) is a normalized lifetime indicator. It starts with 1 for each new cell and ends with zero when the cell reaches the end of life criteria.

When the ESR is chosen to monitor the cell aging, it is expressed by (16).

For the i^{th} storage system cell $i \in [1, n]$, SOH is given by:

$$SOH_i(k+2) = \frac{(2 \cdot ESR_i(0)) - ESR_i(k+2)}{ESR_i(0)} \qquad (16)$$

Finally, the cell's predictive state of aging is represented according to the current solicitations and balancing control.

This final predictive model presented in equation (16) requires information about cells voltage, temperature, current, capacitance and ESR. The voltage, temperature and current measurements are already present thanks to the SCM instrumentation. Indeed, conventional SCM usually monitor each cells thermal and electrical stresses. However, in some cases, individual thermal measurements are not present and supercapacitor temperature could be deduced with a thermal model. The work presented in [37], introduces a simple but efficient thermal model that could be used for example.

The information about capacitance and the ESR is supposed available in this paper. Those parameters evolve very slowly compared to measured data. So, they could be estimated occasionally, online, by the SCM, using observers or some balancing circuit new control [43].

Thus, at each step of time, the predictive model is calibrated with the real measured and estimated supercapacitor stresses and parameters consecutively.

This SOH modeling is the base of the predictive uncommon control strategy.

C. Control objectives

The control of one balancing circuit has only two states, "On" and "Off". So, for n switches, there are 2^n possible switching control sequences. Because of to the predictive model, one sequence is chosen

from the 2^n possible switches sequences. This sequence should satisfy the objectives of the lifetime maximization.

u_i, $i \in [1, 2^n]$ represents the i^{th} control sequences. The possible control states constitute a finite set U as (17).

$$U = [u_1, ..., u_{2^n}] \in [0,1]^n \qquad (17)$$

For energy loss reasons, the last sequence u_{2^n}, where all switches S_i are switched "On", is removed from the space U. Thus, the space of possible control states becomes as in (18):

$$U = [u_1, ..., u_{2^n-1}] \in [0,1]^n \qquad (18)$$

$SOH(u_i)$, with $i \in [1, 2^n-1]$, represents the state of health prediction according to the switches possible sequences.

$$SOH(u_i) = [SOH_1(u_i), ..., SOH_n(u_i)] \in M_{1,n}, i \in [1, 2^n - 1]^n \qquad (19)$$

The aim of the controller is to maximize the lifetime of the energy storage system. The cells having lowest predicted SOH are the weakest cells. They can reach their end of life criterion faster and cause the system's failure. Consequently, the new balancing circuit control strategy tries to reduce the voltage of the weakest cells in order to slow down their deterioration.

So first, the weakest cells are identified. The table J, in equation 20, takes at each time of each sequence $u_i \in U$ the cell having the lowest predicted SOH. Thereafter, one final sequence $u_i \in U$ maximizing the SOH of weakest cells is chosen. The sequence retained is the sequence $u_i \in U$ where J_c is verified (22).

$$J = [J_1, ..., J_n] \in M_{1,n} \quad (20)$$

$$J_i = \min(SOH(u_i)) \in \Re, i \in [1, 2^n - 1] \quad (21)$$

$$J_c = \max(J) \qquad (22)$$

The predictive model based on Eyring law, linear ESR evolution in time could be not perfect. However, the predictive model accuracy doesn't disturb the efficiency of our control. Indeed, the objectives of lifetime maximization are based on the comparison of the state of health predicted. When the same model with same law is used for the whole of the stack elements, its precision level has limited impact.

The conventional equalization requires n memorized variables corresponding to the n cell voltages. It could be represented by a matrix of n lines and 1 column, $M_{(n,1)}$. Indeed, classical balancing circuit control, compares $M_{(n,1)}$ memories, selects the lowest value and orders the energy dissipation in the cells with higher values. The new approach of control requires $((2^n-1) \times n)$ memorized variables,

corresponding to the different states of health prediction according to the 2^n-1 possible sequences of the n switches. It could be represented by a matrix of (2^n-1) lines and n columns, $M_{(2^n-1,\ n)}$. Indeed, the new balancing circuit control, predict the state of health of the $M_{(2^n-1,\ n)}$ memories, compares them in order to identify the lowest cells and select one of the (2^n-1) sequences assuring maximization of predicted state of health of the lowest cells identified.

So thanks to the finite control set model predictive control (FCS-MPC), no complicated optimal resolution algorithm is required but only a largest memory is added. In fact, the same equation (19) is applied for the (2n-1) × n different states and a simple research of maximal and minimal values is applied in order to choose the optimal sequences of control maximizing lifetime. For both control it is important to note that each balancing circuit could be controlled indecently of the others

IV. Performance demonstration

In order to evaluate the FCS-MPC control strategy, realistic simulations are conducted based on a multi model of the supercapacitor's energy storage system.

The simulation is conducted on Matlab/Simulink. It is constituted by a module of supercapacitor storage systems with a dispersion of initial parameters. Each cell evolves in time singularly according to its specific electrical and environmental stresses until failure in order to account for real time behaviors. This storage system is monitored by a supercapacitor management system.

The SCM simulation hardware involves controlled shunting resistors placed at the terminal of each supercapacitor with instrumentations that measure cell's temperature and voltage, storage system's voltage and input current. Software simulation part includes ESR and C estimation along with the switch control. In this paper, the estimations of ESR and C, by estimators or observers are not discussed [43]. This paper focuses only on the control part.

In the following part, the aging of the storage system is studied and analyzed. A comparison of the system's evolution using both new and conventional approaches is developed.

Thus, this section is divided in two subsections: the simulation description and the analysis of the results.

D. Simulation description

The simulation considers an energy storage system including three 3000F, 2.7V supercapacitor models associated in series and three switched shunt 10Ω resistor balancing circuits at the terminal of each cell system. Only three supercapacitors are used in the simulation for simplicity. In fact, three supercapacitors are sufficient to describe the principle of the balancing methods. A maximal temperature dispersion between two elements is applied taking into account transportation application environment.

This storage system undergoes a repetitive power cycling corresponding to a New European Driving Cycle (NEDC) as shown in Fig. 3.

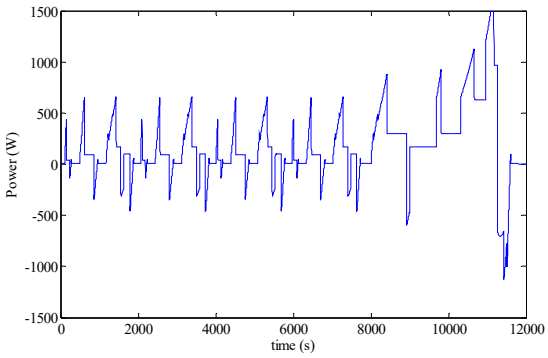


Fig. 3. NEDC power cycle

The simulation used is realistic due to its ability to reproduce different energy storage system real phenomena. In fact, thanks to the different models (electrical, thermal and aging models) used, each supercapacitor simulated, evolves according to its specific solicitations. The thermal model allows supercapacitor overheating reproduction but also the thermal interaction with the ambient temperature. The aging model allows supercapacitor time evolution and according to the electrical and thermal stresses, reproduces the internal parameters degradation in time. Finally, the electrical model interacts with the aging model and evolves in time and use.

Thus every supercapacitor evolves in time according to its own stresses. The energy storage system degrades over time until its failure, driven by the element reaching first, one of its end of life criteria

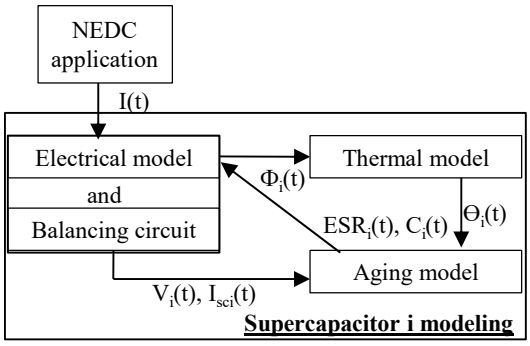


Fig. 4. Supercapacitor cell modeling: I(t) the input current, $V_i(t)$ the terminal cell voltage, $I_{sci}(t)$ the cell current, $\Phi_i(t)$ the effect joule dissipation, $\Theta_i(t)$ the cell temperature.

Figure 4 summarizes the simulation of the supercapacitor's stack model whose parameters are variable according to the application. This diagram represents the coupling realized between different models in order to simulate the real supercapacitor behavior.

The application generates the appropriate current, I(t), according to the power NEDC application and on the measured voltage of the stack.

The supercapacitor electrical model is represented by the simplest but sufficient ESR-C series model.

The aging of each cell is a function of thermal, voltage and cycling stresses as described in the aging model presented above. The lifetime presented in equations (1), (10) and (11) is divided by a factor of 10 in order to reduce the system's lifetime and accelerate the simulation.

To simulate the thermal dynamic behavior of each cell, we used a realistic thermal model which contains the cell overheating and its interactions with the environment.

This thermal model [37], is shown in Fig. 5.

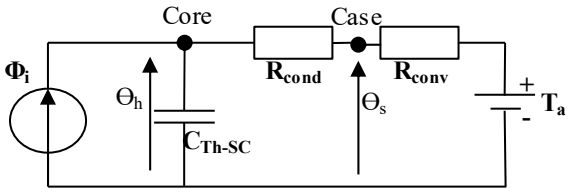


Fig. 5. Thermal model of the supercapacitor

The temperature is represented by two thermal nodes (case and core temperature).

C_{TH-SC} is the thermal capacity of the supercapacitor. It is expressed in Joules per Kelvin.

R_{cond} is the thermal resistance that represents the conduction phenomenon. It is expressed in Kelvins per Watt. It models the heat transfer from the core of the supercapacitor to its case.

R_{conv} is the thermal resistance that represents the convection phenomenon. It is expressed in Kelvins per Watt. It models the temperature exchange between the case and the air.

T_a is the temperature of the external environment. It is expressed in Kelvin.

Φ_i is the heat dissipation from Joule's effect. It is expressed in Watts. It is equal to the supercapacitor's losses during the charge/discharge cycle (reversible heat dissipation [44] is neglected).

E. Results analysis

In this example, the balancing control sample time is 0.1 second corresponding to the NEDC sample time. It is also applied only during charge and rest phases and not in discharge phases in order to minimize energy losses.

The initial parameters of the module cells are summarized in table I.

TABLE I. SIMULATION INITIAL PARAMETERS

	System initial conditions		
	Cell 1	***Cell 2***	***Cell 3***
$C_i(0)$ (F)	3345	3000	2655
$ESR_i(0)$ (mΩ)	0.232	0.261	0.290
$V_i(0)$ (V)	2.5	2.5	2.5
T_{ai} (K)	298	298	298
C_{TH-SCi} (J/K)	700	700	700

	System initial conditions		
	Cell 1	***Cell 2***	***Cell 3***
R_{convi} (kK/W)	0.057	0.059	0.061
R_{condi} (K/W)	0.627	0.627	0.627

For the i^{th} cell: $C_i(0)$ is the initial capacitance, $ESR_i(0)$ is the initial equivalent series resistance, $V_i(0)$ is the initial cell voltage, $C_{TH\text{-}SCi}$, R_{convi} and R_{condi} are respectively the convection capacitance and conduction resistance of the thermal model, T_{ai} is the ambient temperature.

The difference values between each cell has more than one purpose. First of all, it emulates the initial characteristic differences between the supercapacitors in the same stack. A maximal initial dispersion of ±11.5% is setup on the nominal supercapacitor characteristics assigned to the Cell 2. It is secondly used to induce the thermal dispersion that exists across the pack. Thus, both of initial ESR values and the R_{conv} of the thermal model were used to bring a maximum dispersion of ±5°C with the Cell 2 temperature.

Both the balancing circuit classical equalization control and the new lifetime maximization control are applied with these same initial conditions.

The classical equalization approach, which removes charge from the most charged elements, aims to resolve the voltage dispersion between supercapacitors along with the system lifetime. It reduces cell voltages to reach the lowest cell voltage (see Fig. 6).

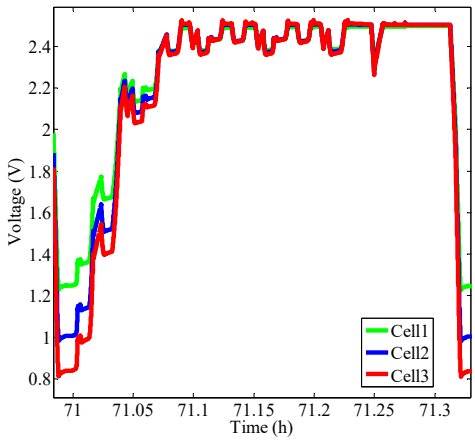


Fig. 4. Cell voltages for NEDC cycle with classical voltage equalization

This new approach identifies at each control step the weakest cells to be less exploited. This one leads voltage dispersion according to aging of the system cells. Figure 7 and 8 represent a case of voltage dispersion observed along the system's lifetime.

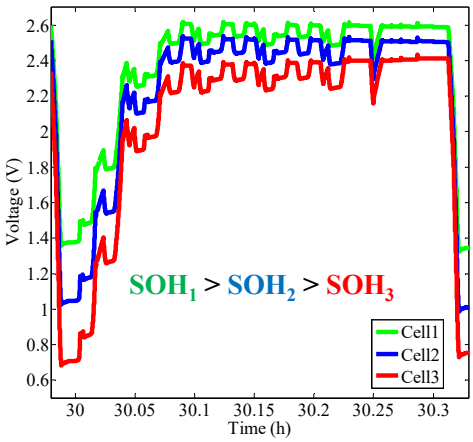


Fig. 5. Case of cell voltages for NEDC cycle with predictive new control.

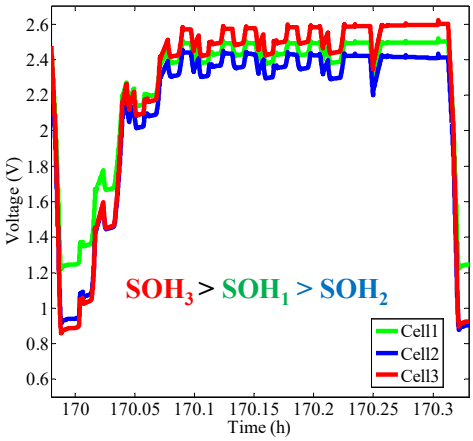


Fig. 6. Case of cell voltages for NEDC cycle with predictive new control

The evolution of the cells $ESR_i(t)$ along the system lifetime is represented in order to analyze its aging behavior according to the balancing circuit control.

Figure 9 represents the evolution of each cell ESR over aging for both balancing control approaches.

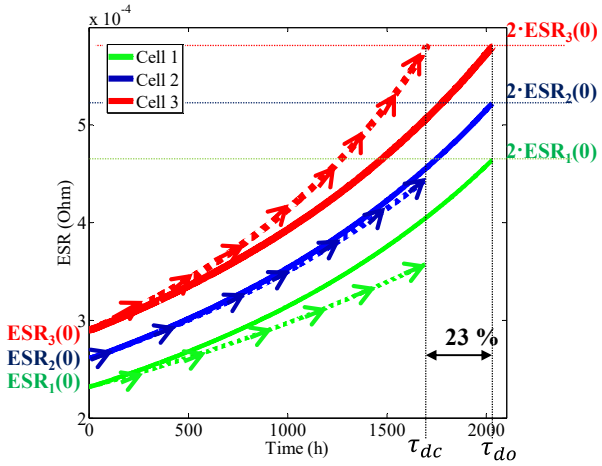


Fig. 7. System ESRi(t) evolution

The full lines represent the cell $ESR_i(t)$ evolution when the new predictive control approach is applied to the system. The dotted lines represent the same cell $ESR_i(t)$ evolution when the classical voltage equalization is applied to the system. The horizontal lines represent the end of life criterion for each supercapacitor. The vertical lines represent the system end of life for each control strategy.

The storage system end of life (noted τ_{dc}) results from the "Cell 3" failure when the conventional voltage equalization is applied. Indeed, this cell, which has the highest ESR and the highest $R_{conv,}$ undergoes a much important thermal stress. Thus, at equal voltages, "Cell 3" is more thermally stressed than other cells so it fails prematurely first.

However, with this new approach of balancing control, the end of life of each cell and consequently of the system is reached at the same time (denoted τ_{do}). Indeed, the new approach compensates the thermal stress by a lower voltage and then equalizes the state of health of the system cell.

Figure 10 represents the system cell's state of health evolution over aging with both control strategies.

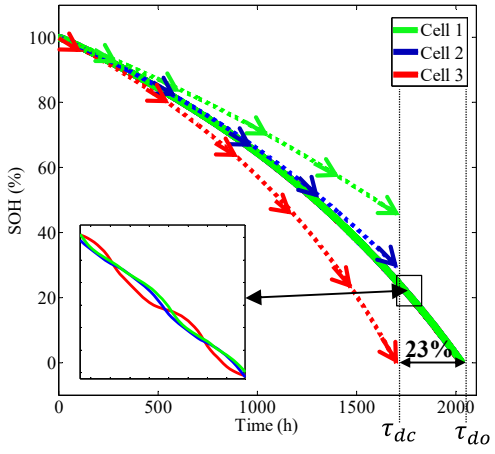


Fig. 8. Cell system SOHi(t) evolution for both control strategies

With the classical equalization and at equal voltages, the weakest element “Cell 3” is aging faster than the others and causes the system’s failure when “Cell 2” has a SOH of 30% and “Cell 1” SOH of 46%. However, with the new approach, the SOH of each cell is equalized in order to maximize the system’s lifetime. The cells reach their end of life criteria simultaneously. Consequently, this method maximizes the storage system’s lifespan and wins more than 23% longevity.

The energy efficiency η is used in the following in order to compare the performances of balancing circuits (23) [17].

$$\eta(\%) = \frac{\sum_{i=1}^{n} W_{sci} - \sum_{i=1}^{n} W_{eqi}}{\sum_{i=1}^{n} W_{sci}} \cdot 100 \qquad (23)$$

Where, W_{sci} is the energy stored in the supercapacitor SC_i along the cycles and W_{eqi} is energy dissipated inside balancing circuit i during cycles.

Table I summarizes the different control strategies resulted from this simulation.

TABLE II. RESULTS COMPARISON

	Classical equalization	***New control***	***Comparison (%)***
End of life t_d(days)	70.7	87.3	+ 23%
Efficiency η (%)	98.8	97.9	- 1%

According to this table, classical equalization dissipated a bit less compared to the new approach of control. Indeed, classical balancing aims to only equalize voltage between elements. So, after a certain period of time, equalization is established and balancing circuit dissipation will be reduced (see Fig.6). However, the new approach of balancing leads to create a voltage dispersion corresponding to the actual dispersion of the state of health. This voltage dispersion changes regularly along SESS lifetime in order to equalize solicitations between supercapacitors (see Fig.7 and Fig.8). Thus, the equalization is never established and the dissipation is more important. However, the difference in balancing efficiencies in both strategies of control doesn’t exceed 1%. So, the system efficiency is considered to be the same in both control approaches. Even if more energy is dissipated in the balancing resistance, the new control approach assures that this dissipation is low compared to the energy stored in the SESS. For example, with a 10 Ω balancing resistance, the maximum current dissipated is 0.27 A. This value is negligible compared to current crossing the supercapacitor for high power solicitations.

F. Lifetime cost

The section before provides the maximization of lifetime of the supercapacitors module and the preservation of the balancing efficiency when the new control of balancing circuit approach is applied. This section is aimed at figuring out the savings behind the reduced costs of this new approach. When

the energy storage reaches its end of life criterion and fails, it is replaced by a new one. The lifetime cost analyses supposes the SCM still working when replacement is made.

We consider in this analyze the same energy storage system, monitored by the same SCM with the same balancing circuits. The only difference is still in the control approach of balancing circuit, which could be the classical voltage equalization or the new approach of control proposed.

The SCM reliability is considered higher than energy storage system reliability. Besides SCM cost still the same whatever is the balancing circuit control used. Thus SCM investment considered as identical, it is neglected in this comparative part.

The indicator used to analyze the system's cost along its usage is Am. It concerns the amortization and used compare the system cost with both balancing control approach (24):

$$Am = \frac{C_s}{\tau_d}[€ / day] \quad (24)$$

C_s is the system cost (25) and $\boldsymbol{\tau}_d$ is the duration of use of the storage system.

$$C_s = n \cdot C_{SC} \quad (25)$$

C_{SC} is the initial investment of 3000F, 2.7V supercapacitors equal to 30€ for each cell corresponding to 10€/kF.

Results of the previous case of simulation with both balancing control strategies are summarized in the table below.

TABLE III. COST COMPARIZON

	Classical equalization	***New control***	***Comparison***
Am (€/day)	1.27	1.03	- 19%

Using same materials and same devices in the same conditions, the storage system longevity is extended by 23% and winning 19% on its amortization. In many high power applications, supercapacitor energy storage system is constituted by dozens and hundreds of serial elements. Thus, winning 19% of the initial investment is considered as a successful result especially when no need to add any special devices to the actual system.

V. Conclusion

This paper presents a new approach of balancing circuit control which enhances the storage system's lifespan. This new approach was never been before. It uses the existing SCM, along with a new kind of balancing circuit control strategy that maximizes the storage system's lifespan. Contrary to conventional balancing function which aims to equalize voltages between system's cells, the new control strategy focuses on the state of aging of each cell. It aims to adapt the solicitation of each cell according to its

state of heath in order to maximize its lifetime and then maximize the whole system's lifespan.

The new control strategy is validated using realistic supercapacitor energy storage system simulation. The simulation represents an energy storage system close to reality monitored by a SCM. It evolves according to its specific solicitations until reaching failure. Comparing a critical case evolution with conventional equalization, the gain is quantified when using this method. The lifetime is extended for this case by 23% with the new control strategy. Moreover, the efficiency of the system remains the same. After that, the price gain is presented when using this new methodology and shows a gain of 19% of the initial investment price by such a control strategy.

The method presented in this paper has many advantages. It uses equipment already present for the majority of storage system applications. It could be implemented in every SCM software and replace conventional voltage equalization strategy. This new approach is studied for the supercapacitor's energy storage systems but it could also be generalized to cover other energy storage systems such as BMS for Li-Ion batteries.

The perspectives of this work are real experiments with real storage system and SCM.

References

[1] J. C. Schroeder and F. W. Fuchs, "General Analysis and Design Guideline for a Battery Buffer System With DC/DC Converter and EDLC for Electric Vehicles and its Influence on Efficiency," *Power Electron. IEEE Trans. On*, vol. 30, no. 2, pp. 922–932, Feb. 2015.

[2] M. Uno and A. Kukita, "Bidirectional PWM Converter Integrating Cell Voltage Equalizer Using Series-Resonant Voltage Multiplier for Series-Connected Energy Storage Cells," *Power Electron. IEEE Trans. On*, vol. 30, no. 6, pp. 3077–3090, Jun. 2015.

[3] A. Kuperman, M. Mellincovsky, C. Lerman, I. Aharon, N. Reichbach, G. Geula, and R. Nakash, "Supercapacitor Sizing Based on Desired Power and Energy Performance," *Power Electron. IEEE Trans. On*, vol. 29, no. 10, pp. 5399–5405, Oct. 2014.

[4] M. Averbukh, S. Lineykin, and A. Kuperman, "Portable Ultracapacitor-Based Power Source for Emergency Starting of Internal Combustion Engines," *Power Electron. IEEE Trans. On*, vol. 30, no. 8, pp. 4283–4290, Aug. 2015.

[5] B. Hredzak, V. G. Agelidis, and G. D. Demetriades, "A Low Complexity Control System for a Hybrid DC Power Source Based on Ultracapacitor–Lead–Acid Battery Configuration," *Power Electron. IEEE Trans. On*, vol. 29, no. 6, pp. 2882–2891, Jun. 2014.

[6] R. German, P. Venet, A. Sari, O. Briat, and J.-M. Vinassa, "Improved Supercapacitor Floating Ageing Interpretation Through Multipore Impedance Model Parameters Evolution," *Power Electron. IEEE Trans. On*, vol. 29, no. 7, pp. 3669–3678, Jul. 2014.

[7] P. Sharma and T. S. Bhatti, "A review on electrochemical double-layer capacitors," *Energy Convers. Manag.*, vol. 51, no. 12, pp. 2901 – 2912, Dec 2010.

[8] D. B. Murray and J. G. Hayes, "Cycle Testing of Supercapacitors for Long-Life Robust Applications," *Power Electron. IEEE Trans. On*, vol. 30, no. 5, pp. 2505–2516, May 2015.

[9] B. Hredzak, V. G. Agelidis, and Minsoo Jang, "A Model Predictive Control System for a Hybrid Battery-Ultracapacitor Power Source," *Power Electron. IEEE Trans. On*, vol. 29, no. 3, pp. 1469–1479, Mar. 2014.

[10] D. B. W. Abeywardana, B. Hredzak, and V. G. Agelidis, "Single-Phase Grid-Connected LiFePO Battery–Supercapacitor Hybrid Energy Storage System With Interleaved Boost Inverter," *Power Electron. IEEE Trans. On*, vol. 30, no. 10, pp. 5591–5604, Oct. 2015.

[11] F. Ongaro, S. Saggini, and P. Mattavelli, "Li-Ion Battery-Supercapacitor Hybrid Storage System for a Long Lifetime, Photovoltaic-Based Wireless Sensor Network," *Power Electron. IEEE Trans. On*, vol. 27, no. 9, pp. 3944 –3952, Sep. 2012.

[12] H. Zhou, T. Bhattacharya, D. Tran, T. S. T. Siew, and A. M. Khambadkone, "Composite Energy Storage System Involving Battery and Ultracapacitor With Dynamic Energy Management in Microgrid Applications," *Power Electron. IEEE Trans. On*, vol. 26, no. 3, pp. 923–930, Mar 2011.

[13] F. A. Inthamoussou, J. Pegueroles-Queralt, and F. D. Bianchi, "Control of a Supercapacitor Energy Storage System for Microgrid Applications," *Energy Convers. IEEE Trans. On*, vol. 28, no. 3, pp. 690–697, Sep. 2013.

[14] A. Affanni, A. Bellini, G. Franceschini, P. Guglielmi, and C. Tassoni, "Battery choice and management for new-generation electric vehicles," *Ind. Electron. IEEE Trans. On*, vol. 52, no. 5, pp. 1343–1349, Oct. 2005.

[15] J. Chatzakis, K. Kalaitzakis, N. C. Voulgaris, and S. N. Manias, "Designing a new generalized battery management system," *Ind. Electron. IEEE Trans. On*, vol. 50, no. 5, pp. 990–999, Oct. 2003.

[16] Jian Qi and D. D.-C. Lu, "Review of battery cell balancing techniques," in *Power Engineering Conference (AUPEC), 2014 Australasian Universities*, pp. 1–6, Sep 2014.

[17] D. Youssef, V. Pascal, and R. Gerard, "Comparison of the Different Circuits Used for Balancing the Voltage of Supercapacitors: Studying Performance and Lifetime of Supercapacitors," presented at the ESSCAP, Lausanne, Suisse, 2006.

[18] M.-Y. Kim, C.-H. Kim, J.-H. Kim, and G.-W. Moon, "A Chain Structure of Switched Capacitor for Improved Cell Balancing Speed of Lithium-Ion Batteries," *Ind. Electron. IEEE Trans. On*, vol. 61, no. 8, pp. 3989–3999, Aug. 2014.

[19] T. H. Phung, A. Collet, and J.-C. Crebier, "An Optimized Topology for Next-to-Next Balancing of Series-Connected Lithium-ion Cells," *Power Electron. IEEE Trans. On*, vol. 29, no. 9, pp. 4603–4613, Sep. 2014.

[20] M.-Y. Kim, J.-H. Kim, and G.-W. Moon, "Center-Cell Concentration Structure of a Cell-to-Cell Balancing Circuit With a Reduced Number of Switches," *Power Electron. IEEE Trans. On*, vol. 29, no. 10, pp. 5285–5297, Oct. 2014.

[21] F. Mestrallet, L. Kerachev, J.-C. Crebier, and A. Collet, “Multiphase Interleaved Converter for Lithium Battery Active Balancing,” *Power Electron. IEEE Trans. On*, vol. 29, no. 6, pp. 2874–2881, Jun. 2014.
[22] Yanqing Qu, Jianguo Zhu, Jiefeng Hu, and B. Holliday, “Overview of supercapacitor cell voltage balancing methods for an electric vehicle,” in *ECCE Asia Downunder (ECCE Asia), 2013 IEEE*, pp. 810–814, Jun 2013.
[23] F. Ibanez, J. Vadillo, J. M. Echeverria, and L. Fontan, “Design methodology of a balancing network for supercapacitors,” in *Innovative Smart Grid Technologies Europe (ISGT EUROPE), 2013 4th IEEE/PES*, pp. 1–5, Oct 2013.
[24] H. K. P. Khant, K. Yamakita, K. Matsui, and M. Hasegawa, “Various voltage equalizers for EDLCs using CW circuit,” in *Industrial Electronics (ISIE), 2013 IEEE International Symposium on*, pp. 1–6, May 2013.
[25] P. Kreczanik, P. Venet, A. Hijazi, and G. Clerc, “Study of Supercapacitor Aging and Lifetime Estimation According to Voltage, Temperature, and RMS Current,” *Ind. Electron. IEEE Trans. On*, vol. 61, no. 9, pp. 4895–4902, Sep. 2014.
[26] R. German, A. Sari, P. Venet, Y. Zitouni, O. Briat, and J.-M. Vinassa, “Ageing law for supercapacitors floating ageing,” in *Industrial Electronics (ISIE), 2014 IEEE 23rd International Symposium on*, pp. 1773–1777, June 2014.
[27] R. German, A. Hammar, R. Lallemand, A. Sari, and P. Venet, “Novel Experimental Identification Method for a Supercapacitor Multipore Model in Order to Monitor the State of Health,” *Power Electron. IEEE Trans. On*, vol. 31, no. 1, pp. 548–559, Jan. 2016.
[28] R. German, A. Sari, P. Venet, O. Briat, and J.-M. Vinassa, “Study of static converters related ripple currents effects on supercapacitors ageing within DC networks,” in *Industrial Electronics (ISIE), 2015 IEEE 24th International Symposium on*, 2015, pp. 1302–1307, June 2015.
[29] P. Azais, L. Duclaux, P. Florian, and D. Massiot, “Causes of supercapacitors ageing in organic electrolyte,” *J. Power Sources*, vol. 171, pp. 1046–1053, Sep 2007.
[30] R. Chaari, O. Briat, J. Y. Deletage, E. Woirgard, and J.-M. Vinassa, “How supercapacitors reach end of life criteria during calendar life and power cycling tests,” *Microelectron. Reliab.*, vol. 51, no. 911, pp. 1976 – 1979, 2011.
[31] T. Kovaltchouk, B. Multon, H. Ben Ahmed, J. Aubry, and P. Venet, “Enhanced aging model for supercapacitors taking into account power cycling: Application to the sizing of an Energy Storage System in a Direct Wave Energy Converter,” in *Ecological Vehicles and Renewable Energies (EVER), 2014 Ninth International Conference on*, 2014, pp. 1–10.
[32] W. Lajnef, J. M. Vinassa, O. Briat, H. E. Brouji, S. Azzopardi, and E. Woirgard, “Quantification of ageing of ultracapacitors during cycling tests with current profile characteristics of hybrid and electric vehicles applications,” *IET Electr. Power Appl.*, vol. 1(5), pp. 683–689, 2007.
[33] H. E. Brouji, O. Briat, J. M. Vinassa, N. Bertrand, and E. Woirgard, “Impact of calendar life and cycling ageing on supercapacitor performance,” *IEEE Trans. Veh. Technol.*, vol. 58, pp. 3917–3929, 2009.
[34] T. Geyer and D. E. Quevedo, “Multistep Finite Control Set Model Predictive Control for Power Electronics,” *Power Electron. IEEE Trans. On*, vol. 29, no. 12, pp. 6836–6846, Dec. 2014.
[35] Sangshin Kwak and Jun-Cheol Park, “Switching Strategy Based on Model Predictive Control of VSI to Obtain High Efficiency and Balanced Loss Distribution,” *Power Electron. IEEE Trans. On*, vol. 29, no. 9, pp. 4551–4567, Sep. 2014.
[36] S. Vazquez, J. I. Leon, L. G. Franquelo, J. Rodriguez, H. A. Young, A. Marquez, and P. Zanchetta, “Model Predictive Control: A Review of Its Applications in Power Electronics,” *Ind. Electron. Mag. IEEE*, vol. 8, no. 1, pp. 16–31, Mar. 2014.
[37] A. Hijazi, P. Kreczanik, E. Bideaux, P. Venet, G. Clerc, and M. Di Loreto, “Thermal Network Model of Supercapacitors Stack,” *Ind. Electron. IEEE Trans. On*, vol. 59, no. 2, pp. 979–987, Feb. 2012.
[38] R. Chaari, O. Briat, and J.-M. Vinassa, “Capacitance recovery analysis and modelling of supercapacitors during cycling ageing tests,” *Energy Convers. Manag.*, vol. 82, no. 0, pp. 37–45, Jun. 2014.
[39] R. Chaari, O. Briat, J. Y. Deletage, R. Lallemand, J. Kauv, G. Coquery, and J.-M. Vinassa, “Ageing quantification of supercapacitors during power cycling using online and periodic characterization tests,” in *Vehicle Power and Propulsion Conference (VPPC), 2011 IEEE*, 2011, pp. 1–5.
[40] A. Hammar, P. Venet, R. Lallemand, G. Coquery, and G. Rojat, “Study of Accelerated Aging of Supercapacitors for Transport Applications,” *Ind. Electron. IEEE Trans. On*, vol. 57, no. 12, pp. 3972 –3979, Dec. 2010.
[41] R. German, A. Sari, P. Venet, O. Briat, and J.-M. Vinassa, “Study on specific effects of high frequency ripple currents and temperature on supercapacitors ageing,” *Proc. 26th Eur. Symp. Reliab. Electron Devices Fail. Phys. Anal. ESREF 2015*, vol. 55, no. 9–10, pp. 2027–2031, Aug. 2015.
[42] M. Ayadi, O. Briat, R. Lallemand, A. Eddahech, R. German, G. Coquery, and J. . Vinassa, “Description of supercapacitor performance degradation rate during thermal cycling under constant voltage ageing test,” *SI ESREF 2014*, vol. 54, no. 9–10, pp. 1944–1948, Sep. 2014.
[43] S. Shili, A. Hijazi, P. Venet, A. Sari, Xuefang Lin-Shi, and H. Razik, “Balancing circuit control for supercapacitor state estimation,” in *Ecological Vehicles and Renewable Energies (EVER), 2015 Tenth International Conference on*, 2015, pp. 1–7.
[44] J. Schiffer, D. Linzen, and D. U. Sauer, “Heat generation in double layer capacitors,” *J. Power Sources*, vol. 160, no. 1, pp. 765 – 772, 2006.